

## Thermally Assisted Magnetization Reversal in Submicron-Sized Magnetic Thin Films

R. H. Koch, G. Grinstein, G. A. Keefe, Yu Lu, P. L. Trouilloud, and W. J. Gallagher

*IBM Thomas J. Watson Research Center, Yorktown Heights, New York 10598*

S. S. P. Parkin

*IBM Almaden Research Center, Almaden, California 95120*

(Received 27 December 1999)

We have measured the rate of thermally assisted magnetization reversal of submicron-sized magnetic thin films. For fields  $H$  just less than the zero-temperature switching field  $H_C$ , the probability of reversal,  $P_s^{\text{exp}}(t)$ , increases for short times  $t$ , achieves a maximum value, and then decreases exponentially. Micromagnetic simulations exhibit the same behavior and show that the reversal proceeds through the annihilation of two domain walls that move from opposite sides of the sample. The behavior of  $P_s^{\text{exp}}(t)$  can be understood through a simple “energy-ladder” model of thermal activation.

PACS numbers: 75.70.Ak, 75.50.Tt

The growing importance of high-speed magnetoelectronics [1] has encouraged a large and growing effort to understand the dynamics of magnetization reversal in submicron-sized magnetic thin films. Magnetization reversal is simply the reversal of the direction of the magnetic moment of a magnetized sample caused by applying a magnetic field in the direction opposite to the moment. Most of the existing studies of this phenomenon have examined the situation wherein a pulsed magnetic field greatly exceeding the value of the zero-temperature ( $T = 0$ ) switching field,  $H_C$ , is applied, whereupon the reversal appears to begin immediately and finishes in a few nanoseconds or less. Many theoretical and experimental reports [2–4] have convincingly demonstrated the validity of micromagnetic modeling, based on the Landau-Lifshitz-Gilbert (LLG) equations, for describing magnetization reversal in small systems under these conditions.

An equally important regime for magnetization reversal is one wherein the applied field is less than  $H_C$ . In the classical picture at  $T = 0$ , the magnetization does not reverse with the field for  $H < H_C$ , but remains stuck in a metastable local energy minimum. At  $T > 0$ , thermal energy allows the film to escape this minimum by climbing the energy barrier and finding the global energy minimum of the reversed state. This process has been studied on length scales ranging from molecular [5] to macroscopic, where it is connected with magnetization creep [6]. Recent experiments on individual particles of size 10–300 nm [7–9] have been designed to test the Néel-Brown [10] model for thermal activation of single-domain ferromagnets over an energy barrier. In this model, the probability  $P_s(t)$  for the magnetization to switch sign decays like  $e^{-t/\tau}$ , the relaxation time  $\tau$  obeying the Arrhenius law,  $\tau = \tau_0 e^{U/k_b T}$ , where  $\tau_0$  is a microscopic attempt time and  $U$  the barrier height. The experiments were found to be consistent with an exponential switching probability for the smallest particles [8,11], but inconsistent for larger particles [7].

This paper reports the first experimental study of thermally assisted magnetization reversal in submicron-sized

thin films [12]. Our experiment prepares a submicron film in a metastable state with the applied field close to but less than  $H_C$ , and measures the time it takes the film to switch into the energetically preferred reversed state, where the magnetization and applied field are aligned. We have systematically studied the reversal as a function of applied field and temperature for many samples. We find that the switching probability  $P_s^{\text{exp}}(t)$  initially *increases* with time, eventually achieving a maximum value, after which it decays exponentially.

Such peaks in switching probabilities have not previously been observed in magnetic systems. They have, however, been reported in Monte Carlo simulations of 1D micromagnetic models [13] and 2D Ising models [14]. Here we rationalize the occurrence of such peaks quite generally on the basis of a simple one-variable “energy-ladder model,” wherein the system climbs an energy barrier through thermal activation up a ladder of states of increasing energy. We have also modeled the films micromagnetically, using finite element LLG calculations. These simulations produce the same qualitative phenomenology as do the experiments and the energy-ladder model, and provide a picture of the detailed microscopics of the thermally assisted reversal process.

The sample consisted of two thin ferromagnetic films separated by an  $\text{Al}_2\text{O}_3$  tunnel junction [15]. The bottom film, the “pinned layer,” was antiferromagnetically pinned in the easy (long) axis direction of the film. The top film, the “free layer,” was a 5 nm layer of either  $\text{Ni}_{60}\text{Fe}_{40}$ , or permalloy. The structures reported here were all hexagons, elongated so as to look like rectangles with pointed ends. They are  $0.3 \mu\text{m}$  by  $0.8 \mu\text{m}$  in size, though different size samples were also tested. The sample resistance varied from 1 to 50 k $\Omega$ . Immediately above and below each magnetic tunnel junction were aluminum thin film cross stripes, used to measure the tunnel junction resistance and to apply an easy axis magnetic field to switch the magnetization direction of the free layer. For the small fields applied in this experiment, the pinned layer magnetization direction

does not change. Spin-polarized tunneling between the two magnetic layers provides a magnetoresistance effect in the range of 10% to 30%, which was used as a simple probe of the easy axis component of free layer magnetization.

We measured the samples in either a room-temperature setup, or a variable-temperature setup that uses a regulated-temperature sample holder with a temperature range from 77 K to room temperature. After each sample was fabricated, we measured the dc magnetization-field (M-H) loops for a number of hard axis bias fields. Each sample we measured was first voltage biased across the junction with a small dc voltage of about 0.1 V. In order to measure one reversal time, we first reset the sample with a long duration easy axis magnetic field pulse of about  $-200$  Oe. At a time we take as  $t = 0$ , we then applied a positive magnetic field step to bias the sample near or just below the switching field,  $H_C$ . This field step was applied to the junction using the thin film easy axis bias line running across the junction, which was driven by the current from a pulse generator via a  $50 \Omega$  coaxial line. The rise time of the pulse is about 3 ns for the room-temperature setup, and somewhat longer for the variable-temperature setup.

After some waiting time,  $t$ , the free layer magnetization reversed, changing the resistance of the sample and producing a current pulse through the junction. This current pulse induced a voltage pulse in a coaxial cable leading from the junction. In order to measure a distribution of switching times, this process—reset, pulse, wait, and measure—was typically repeated 10 000 times for each value of the easy and hard axis applied fields. (The hard axis field was 1.0 Oe throughout.)

The measured distribution of switching times,  $P_s^{\text{exp}}(t)$ , for one of the more than ten samples we studied, is shown in Fig. 1(a). When the sample was pulse biased at or just below  $H_C$  (about 80 Oe for this sample), the time to switch was very short, as shown by the heavy patch of solid lines on the plot for  $t < 0.1 \mu\text{s}$ . As the pulsed bias was decreased to 1 to 2 Oe below  $H_C$ , a clear peak in  $P_s^{\text{exp}}(t)$  appeared at larger  $t$ . As  $H - H_C$  was decreased further (to  $-10$  Oe), this peak became broader and moved out to later times. Beyond the peak, the switching probability decayed exponentially with time.

Two times can be defined from these plots:  $\tau_P$ , where the peak in the switching probability occurs; and the decay time  $\tau_D$ , determined by fitting  $P_s^{\text{exp}}(t)$  to the exponential form  $e^{-t/\tau_D}$  for  $t > \tau_P$ . One can also define an activation energy  $E_{\text{ACT}}$  corresponding to  $\tau_D$  via the relation  $\tau_D = \tau_0 \exp(E_{\text{ACT}}/k_B T)$ , where  $\tau_0$  is a characteristic attempt time. As explained below,  $\tau_0$  was inferred to be roughly  $0.2 \mu\text{s}$ .

For any given  $T$ , we then define  $H_C$  operationally as the field where  $E_{\text{ACT}}$  extrapolates to 0 on an  $E_{\text{ACT}}$  vs  $H$  plot. Since the material properties of the junctions change with temperature, the  $H_C$ 's determined in this way vary with  $T$ . However, the  $E_{\text{ACT}}$  vs  $H$  curves for different  $T$ 's and different junctions all look quite linear [16], and their

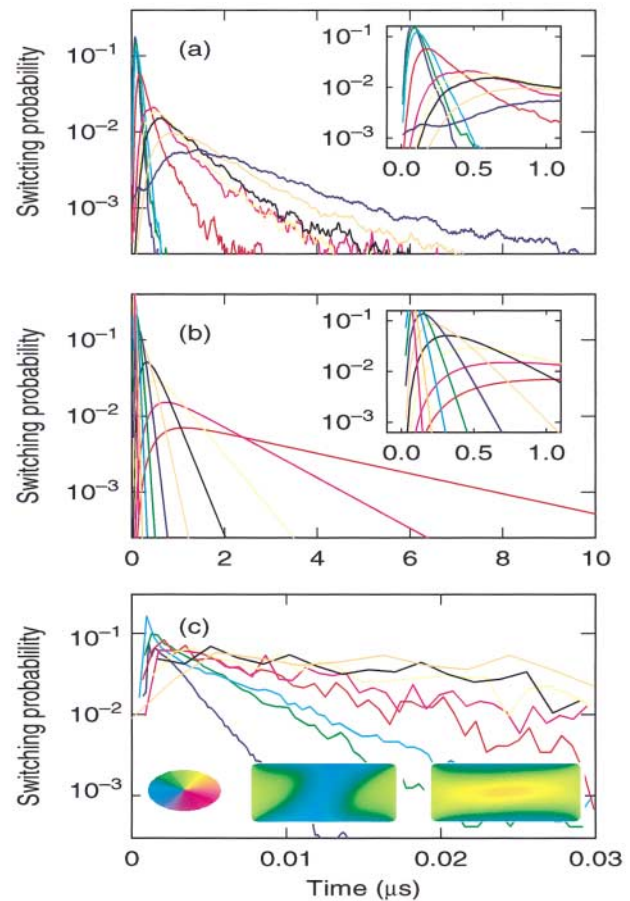


FIG. 1 (color). (a) Measured switching probability vs time, for one sample at 300 K, for a number of different values of  $H_C - H$  between 1 and 6 Oe. Inset is a blowup of the same data near  $t = 0$ . (b) Predicted switching probability vs time from the energy-ladder model for  $N = 4$ ,  $q = 0.001$ , and for a range of  $p$  values. Inset is a blowup of the same data near  $t = 0$ . (c) Predicted switching probability vs time from the micromagnetic simulation of a rectangular sample at 300 K, averaged over 1000 switching events. Insets show the magnetization direction in the sample for a typical run before (left panel) and after (right panel) the switch.

slopes are all essentially the same. Thus, plotted against  $H_C - H$  (Fig. 2), all the  $E_{\text{ACT}}$  data lie roughly on one straight line. At the lowest temperatures, the flattening of the curves near  $H_C - H = 0$  results from the finite response time of the variable-temperature setup. An activation energy of  $0.3 \times 10^{-20}$  J corresponds to a decay time of about  $3 \mu\text{s}$ , which cannot be resolved in this setup.

Figure 3 plots the measured values of  $\tau_P$  vs  $\tau_D$  for seven junctions at  $T = 300$  K. For the shortest times,  $\tau_P$  exceeds  $\tau_D$ . As  $H_C - H$  is increased, both times increase, and eventually  $\tau_P$  becomes significantly less than  $\tau_D$ . The data lie roughly on one sample-independent curve.

Figures 1(a) and 1(c) show that simulations using the LLG model produce switching probabilities qualitatively consistent with the data. The simulations, performed on rectangular samples with disorder in the anisotropy which

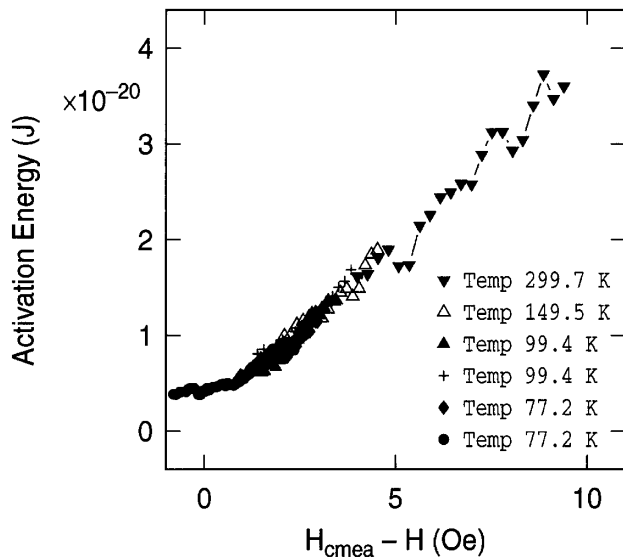


FIG. 2. Measured activation energy vs  $H_C - H$  for four temperatures and two samples.

approximates NiFe, also provide information about the nature of the switching process: Two domain walls [see Fig. 1(c), top inset] move stochastically, uphill in energy, from opposite ends of the sample, eventually annihilating near the center and causing the switch, whose aftermath is shown in the bottom inset. One is limited numerically to studying switching for small energy barriers, resulting in switching times comparable to the shortest times in our experiments. Moreover, the LLG model provides little insight into why the  $P_s^{\text{exp}}$  curves look the way they do. Thus we have abstracted the switching further, and analyzed

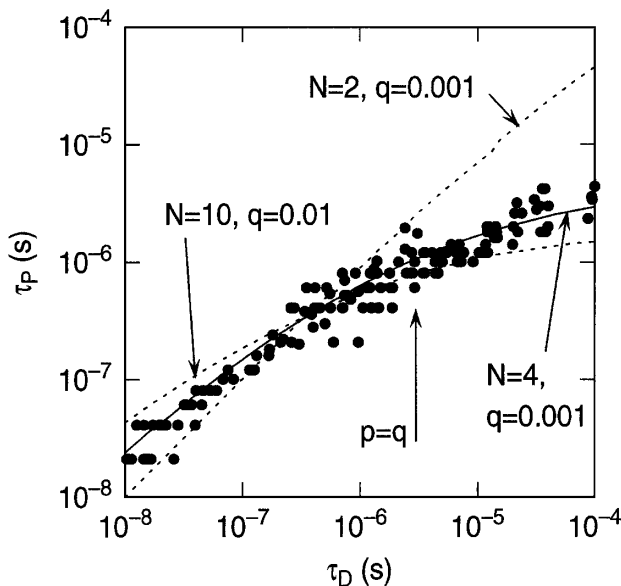


FIG. 3. Measured values of  $\tau_P$  vs  $\tau_D$  for seven samples at 300 K. The solid and dashed lines are predictions from the energy-ladder model for the indicated values of  $N$  and  $q$ .

an elementary energy-ladder model that seeks to capture the main physics of the thermal activation over a barrier by generalizing the Poisson switching of the Néel-Brown model to a many-step process.

The model consists of a single degree of freedom or “particle” that occupies any one of  $N$  states,  $i = 1, 2, \dots, N$ , with energies  $E_i$  that increase by a constant amount,  $\Delta E$ :  $E_i = i\Delta E$ . Starting from the lowest state,  $i = 1$ , at time  $t = 0$ , the particle climbs stochastically, via thermal activation, up the ladder of states, eventually escaping from the system altogether or “switching.” This process [17] is designed to mimic the motion of the domain walls in our magnetic films [Fig. 1(c), upper inset]. It could, however, be taken to represent schematically almost any activated process, such as the growth, through a series of intermediate configurations of increasing radii and energy, of a droplet of the stable phase in a metastable system [13,14]. When the critical droplet radius is achieved, the system switches rapidly into the stable phase.

The dynamical rules of the model are as follows: From state  $i$  at time  $t$ , the particle can, at time  $t + 1$ : (1) move to state  $i + 1$ , (2) move to state  $i - 1$ , (3) escape from the system, or (4) remain in state  $i$ , with respective probabilities  $p_i, q_i, r_i$ , and  $1 - p_i - q_i - r_i$ ; thus  $p_i + q_i + r_i \leq 1$  for all  $i$ . Obviously  $q_1 = p_N = 0$ , and for simplicity [18] we take  $p_i = p$  and  $r_i = 0$  for all  $i < N$ ,  $q_i = q$  for all  $i > 1$ , and  $r_N = p$ . For  $N = 1$  one recovers the exponential switching of the Néel-Brown model.

These rules can be cast as a master equation [17] for the probability  $P_i(t)$  of finding the model in state  $i$  at time  $t$ :  $P_i(t + 1) = \sum_j W_{ij} P_j(t)$ , where the transition matrix  $W$  depends simply on the parameters. This equation can be solved analytically for small  $N$ , and numerically for all  $N$ . For large  $t$ , the escape or switching probability,  $P_s(t)$ , decays exponentially:  $P_s(t) \sim e^{-t/\tau_D}$ , with some characteristic time  $\tau_D$ . For small  $t$ , however,  $P_s(t)$  typically increases with time, reflecting the gradual buildup of probability in the higher energy states from which escape is easiest. For all  $N \geq 2$ ,  $P_s(t)$  can therefore exhibit a peak at a second characteristic time,  $\tau_P$ . One can show that as  $p \rightarrow 0$  for fixed  $q$ ,  $\tau_D$  diverges like  $1/p^N$  and  $\tau_P$  diverges weakly, like  $\ln(\tau_D)$ , i.e., like  $\ln(1/p)$ . This limit, where the particle moves upward in energy very slowly, corresponds to  $H \ll H_C$  in the experiments.

The energy-ladder model provides a plausible picture for the occurrence of the peak in the experimental  $P_s^{\text{exp}}(t)$ , the notion being that it takes time for the domain walls to climb the energy barrier until they are close enough together that the switching probability becomes significant. The exponential decay of  $P_s^{\text{exp}}(t)$  for  $t > \tau_P$  conforms to the behavior of the model as well. It is also relatively easy to find model parameters that produce results in reasonable quantitative agreement with the observations. Note that detailed balance implies  $p/q = e^{-\Delta E/k_B T}$ . We took  $N$  and  $q$  as adjustable parameters, while  $p$  was varied to change

the height of the energy barrier, hence mimicking the role of the magnetic field in the experiments [19].

For a given  $q$ , one can assign a physical time interval to one time step in the model by noting that the exact solution for  $\tau_D$  in the limit  $p/q \rightarrow 0$  is  $\tau_D = q^{N-1}/p^N = e^{U/k_B T}/q$ , where  $U = N\Delta E$  is the total energy barrier. Recalling that  $\tau_D = \tau_0 e^{U/k_B T}$  for our films when  $U \gg k_B T$ , we conclude that  $1/q = \tau_0$ . Thus each time step in the model represents the time interval  $q\tau_0$ . By matching the  $\tau_P$  vs  $\tau_D$  curve from the model to the experimental data of Fig. 3, one then obtains an estimate for  $\tau_0$ . We performed this match for a given  $N$  and  $q$  by finding numerically the value of  $p$  for which  $\tau_P = \tau_D$  in the model, and setting this time equal to  $3 \times 10^{-7}$  s—the time for which  $\tau_P = \tau_D$  in Fig. 3.

The shapes of both the  $P_s(t)$  and  $\tau_P$  vs  $\tau_D$  curves from the model vary substantially with  $N$  and  $q$  (see Fig. 3). The best match between the model and the experimental data is obtained for  $N = 4$  and  $q \sim 0.001$ , where the agreement is good [Figs. 1(a), 1(b), and 3]. The estimate,  $\tau_0 \sim 0.2 \mu\text{s}$ , obtained from  $N = 4$  and  $q = 0.001$  is considerably larger than the subnanosecond time scales typical of microscopic attempt times. However,  $\tau_0$  should be thought of as the time it takes a domain wall segment to diffuse through a characteristic distance—its own width of a few lattice spacings, say—rather than to a single-spin-flip time. Thus  $\tau_0$  reflects the collective dynamics of many spins. Though one should not attach undue significance to the comparison between the ladder model and the data, one can ask why values of  $N$  as small as 4 provide a better match to the data than  $N$ 's larger than 10, say. The answer may be that the physical samples are disordered to some extent, owing to fluctuations in local anisotropy strength, edge roughness, etc. The disorder likely produces sites that pin domain walls, whose motion can then be pictured as jumps between neighboring pinning positions, each of which is a local minimum of the energy. In this interpretation, each pinning position can be thought of as a state of the ladder model. One would then expect  $N$  to be modest, since the samples are so small.

Thus we postulate that in the experimental system a local energy barrier separates any two adjacent pinning positions. This is represented in the ladder model by the transition probabilities  $p$  and  $q$  (which connect adjacent states  $i$  and  $i + 1$ ) being, respectively, proportional to  $e^{-(\Delta E + E_B)/k_B T}$  and  $e^{-E_B/k_B T}$ , where  $E_B (> 0)$  is the local barrier due to pinning, and  $\Delta E$  is the field-dependent slope of the energy landscape [19]. Thus far we have been thinking of  $\Delta E$  as positive, i.e., of  $p < q$ , which is certainly true when  $H$  is sufficiently less than  $H_C$ . At  $H_C$ , however, the total energy barrier to hopping from state  $i$

to state  $i + 1$  must vanish, so that  $\Delta E = -E_B < 0$ , or  $p > q$ . At the point  $p = q$  (indicated by the arrow in Fig. 3),  $\Delta E = 0$ , so that the energy landscape has zero net slope, all states having the same energy. In our magnetic films, this point corresponds to the field value where a domain wall can move to the left or to the right with equal probability.

We thank D. Abraham, S. Ingvarsson, C. Jayaprakash, J. Krug, N. Rizzo, T. Silva, and G. Xiao for helpful suggestions. This work was supported in part by the Defense Advanced Research Projects Agency, Contract No. MDA972-99-C-0009.

- 
- [1] Special Issue on Magnetoelectronics [Phys. Today **48**, No. 4, 24 (1995)].
  - [2] T. M. Crawford, T. J. Silva, C. W. Teplin, and C. T. Rogers, Appl. Phys. Lett. **74**, 3386 (1999).
  - [3] W. K. Hiebert, A. Stankiewicz, and M. R. Freeman, Phys. Rev. Lett. **79**, 1134 (1997).
  - [4] R. H. Koch *et al.*, Phys. Rev. Lett. **81**, 4512 (1998).
  - [5] For example, A. D. Kent *et al.*, Europhys. Lett. **49**, 521 (2000).
  - [6] For example, Y. B. Kim and M. J. Stephen, in *Superconductivity*, edited by R. D. Parks (Dekker, New York, 1969), Vol. 2, p. 1107.
  - [7] M. Lederman, S. Schultz, and M. Ozaki, Phys. Rev. Lett. **73**, 1986 (1994); M. Lederman *et al.*, J. Appl. Phys. **75**, 6217 (1994).
  - [8] W. Wernsdorfer *et al.*, Phys. Rev. Lett. **78**, 1791 (1997); W. Wernsdorfer *et al.*, Phys. Rev. Lett. **79**, 4014 (1997).
  - [9] W. T. Coffey *et al.*, Phys. Rev. Lett. **80**, 5655 (1998).
  - [10] L. Néel, Ann. Geophys. **5**, 99 (1948); W. F. Brown, Jr., Phys. Rev. **130**, 1677 (1963).
  - [11] W. Wernsdorfer *et al.*, Phys. Rev. Lett. **77**, 1873 (1996).
  - [12] For studies of larger thin films, see, e.g., J. Pommier *et al.*, Phys. Rev. Lett. **65**, 2054 (1990).
  - [13] J. M. González *et al.*, Phys. Rev. B **52**, 16034 (1995).
  - [14] H. L. Richards *et al.*, J. Magn. Magn. Mater. **150**, 37 (1995); D. García *et al.*, J. Appl. Phys. **79**, 6019 (1996).
  - [15] W. J. Gallagher *et al.*, J. Appl. Phys. **81**, 3741 (1997).
  - [16] For  $H_C - H \rightarrow 0$ ,  $E_{\text{ACT}} \sim (H_C - H)^{3/2}$  in general. See R. H. Victora, Phys. Rev. Lett. **63**, 457 (1989).
  - [17] Models of this type—"one-step processes with an absorbing boundary"—are discussed in N. G. Van Kampen, *Stochastic Processes in Physics and Chemistry* (North-Holland, Amsterdam, 1981), Chap. VI.
  - [18] Generalization to nonuniform  $p_i$ ,  $q_i$ ,  $r_i$ , and  $\Delta E$ , and/or to continuous time, is trivial.
  - [19] One could also change  $\Delta E$  by varying both  $p$  and  $q$  consistent with  $p/q = e^{-\Delta E/k_B T}$ .